Synthesis of Magnetic Chitosan Hydrogel from crab shells as an Environmentally-friendly Adsorbent for Water Purification

Ethan John Lim 4S1, Yu Zhenning 4S2, Fu Wenbo 4S3

Group 1-46

Abstract

Water pollution is a serious problem in the world. Crab shells are abundant biowastes which can be harnessed to produce useful chitosan. In this project, chitosan was synthesised from chitin extracted from crab shells. The degree of deacetylation and molecular weight of chitosan synthesised were determined by Fourier Transformation Infra-red Spectroscopy (FTIR) and mass spectrophotometry respectively. Two different methods of Magnetic Chitosan Hydrogel (MCH) synthesis were explored based on the molecular weight of chitosan used. Chitosan synthesized in this study had low molecular weight while commercial chitosan has high molecular weight. Chitosan of low molecular weight was converted to MCH by sodium hydroxide precipitation while high molecular weight commercial chitosan was converted to MCH via ethanol precipitation. Both MCHs were as effective as commercial activated carbon (AC) in removing direct red and acid blue dye, and outperformed commercial AC in removing methyl orange. The maximum adsorption capacities of MCH synthesised from chitosan and commercial chitosan on direct red and acid blue were higher than that of several adsorbents reported in literature. Kinetic studies also reveal fast adsorption rates of both MCH in removing the dyes, with both adsorbents being able to achieve 90% removal for both dyes within 15 minutes. Unique magnetic property of both MCH renders them reusable while sustaining more than 90% removal of acid blue even after 5 cycles. MCH is a promising and environmentally-friendly adsorbent which is able to remove dyes rapidly from water.

1. Introduction

Industries are the major sources of pollutants in all environments and various levels of pollutants are being discharged into the environment either directly or indirectly (Ado et al., 2015). Many industries such as the textile industry utilise dyes to colour their products. However, 50% of the dyes used are lost and discharged in wastewater due to the low levels of dye-fibre fixation (Mohan, Balasubramanian & Basha., 2007). The removal of dyes from wastewater discharge has become increasingly important as even a small quantity of dye in water can be toxic and highly visible (Malik, Ramteke & Wate., 2007). Discharge of these dyes into water sources affects the people who may use these sources for living purposes such as washing, bathing and drinking (Sharma & Sobti, 2000). Dyes may impart toxicity to aquatic

life and are found to be mutagenic, carcinogenic and may cause severe damage to organs (Kadirvelu et al., 2003). Dyes can also deleteriously affect aquatic plants because they inhibit the penetration of sunlight into the receiving water bodies (Shen et al., 2009). Due to the environmental challenges that dyes pose and the imposition of government legislation requiring textile wastewater to be treated, there is a significant demand for an effective solution to remove such dyes from wastewater.

To solve this problem, ultrafiltration, nanofiltration and hyperfiltration were investigated to recover the dyes and chemicals from industrial wastewater (Avlonitis, Poulios, Sotiriou, Pappas, & Moutesidis., 2008). Although these methods are efficient, they are very costly and commercially unattractive (Sulak, Demirbas & Kobya, 2007). Adsorption has been found to be superior to other techniques for water reuse in terms of manufacturing cost, speed, ease of operation and insensitivity to toxic pollutants (Crini & Badot, 2008). However, many of the current adsorbents, such as activated carbon, are limited by the high costs involved in both the precursors and the production process (Srivastava, Mall & Mishra, 2007). Thus, there is an urgent need for the production of highly efficient and cost-effective adsorbents for dye removal.

Chitosan is a type of natural polyaminosaccharide obtained from chitin partial deacetylation; it is the second-most abundant polymer in nature after the lignocellulose group (Ngah, Teong & Hanafiah, 2011). Chitosan can be derived from crustacean shells such as crab shells, an undesirable by-product of the food industry (Ngah & Isa, 1998). The high chitin content of crab shells (Toliba., Rabie & El-Araby,, 2014) renders it a suitable precursor for the extraction of chitin and the subsequent production of chitosan from it. The food industry generates 6 million to 8 million tonnes of crustacean shells every year (Drahl, 2019). A large proportion of the wastes are either burnt or jettisoned in landfills, which perpetuates environmental problems.

The carbohydrate backbone of chitosan is very similar to that of cellulose; with the hydroxyl at position C-2 replaced by an amino group. Chitosan, which is a kind of cationic cellulose derivative, displays a high adsorption capacity for many types of dyes. However, powdery chitosan has some disadvantages that limit its use in practical applications. It is soluble in acids and has poor mechanical strength. In addition, the separation and recovery of chitosan powder is still problematic for researchers (Zhu et al., 2010).

In this study, a fast and highly efficient method for the removal of dyes using magnetic chitosan-Fe(III) hydrogel, synthesised with cheap and environmentally friendly chitosan from crab shell was proposed. The use of crab shells could potentially reduce the cost of the hydrogel

and at the same time alleviate the impacts that these waste crab shells pose to the environment. Magnetising the hydrogel renders the separation of the hydrogel from treated wastewater convenient and effective.

2. Objectives and Hypothesis

This study aims to extract chitin from crab shells and convert it to chitosan. The chitosan produced in this study is of low molecular weight, and was converted to magnetic chitosan hydrogel (MCH) via NaOH precipitation and is designated MCH-N. On the other hand, commercial chitosan with high molecular weight was converted to MCH via ethanol precipitation for comparison and is designated as MCH-E. The effectiveness of both MCHs in removing anionic dyes (acid blue, direct red and methyl orange) was compared with commercial activated carbon. The reusability of both MCHs over several cycles was also evaluated and compared.

This study hypothesizes that Magnetic Chitosan Hydrogel (MCH) will be successfully synthesised from chitin extracted from crab shell. The effectiveness of both MCHs in removing anionic dyes will be comparable to commercial activated carbon. Both MCHs will be able to sustain their effectiveness in dye removal for at least 5 cycles.

3. Materials and Methods

3.1 Materials

Crab shells of species *Scylla serrata* were obtained from coffeeshop. Sodium hydroxide, trisodium citrate, iron(II) sulfate and iron(III) chloride were procured from GCE Chemicals. Direct red , acid blue and methyl orange dyes were procured from Sigma Aldrich.

3.2 Extraction of Chitin and synthesis of Chitosan from Crab Shells

There are 3 main components in this process: Demineralisation, Deproteinization and Deacetylation. Demineralization of the crab shells was carried out with 3% (v/v) HC*l* at room temperature with a solid to solvent ratio of 1:5 (w/v) for 8 hours. The residue was washed until neutral pH. Deproteinization of the crab shells was carried out with 4% (w/v) NaOH at room temperature with a solid to solvent ratio 1:5 (w/v) for 20 hours. The residue was washed until neutral pH. Purified chitin was then dried and ground to small particles to facilitate deacetylation. Deacetylation of chitin was carried out using 10M NaOH at 65°C with a solid to solvent ratio of 1:10 (w/v) for 20 hours. Acetic acid was added to dissolve the chitosan, after which the mixture was centrifuged, and NaOH was added until pH 12. The mixture was then

centrifuged and the obtained chitosan was washed, dried and ground. It was then washed until pH neutral and dried.

3.3 Determination of Degree of Deacetylation (%DDA) of Chitosan Synthesised by Fourier Transform Infrared Spectroscopy (FTIR)

During the process of deacetylation, the acetyl group present in chitin is removed, converting the amide functional group (-CO-NH) into an amine ($-NH_2$). Therefore, by taking the ratio of the absorbance reading of the amide group (changed during deacetylation) at 1655 cm^{-1} to the reading of the hydroxyl group (unchanged during deacetylation) at 3450 cm^{-1}, the percentage of deacetylation (DDA) of the chitosan synthesized can be determined by the following formula:

$$DDA(\%) = [1- (A_{1655}/ A_{3450})/1.33] \times 100$$

The ratio of 1.33 represents the ratio of A_{1655}/ A_{3450} for fully N-acetylated chitosan.

3.4 Synthesis of Magnetite Nanoparticles (NPs)

For the synthesis of Magnetite NPs, iron(II) and iron(III) ions have to be present in the solution with a molar ratio of 1:2. Therefore, 3.87 g of iron(II) sulfate and 7.97 g of iron(III) chloride were dissolved in 50 ml of deionized water and heated to 80 °C and stirred for 30 min. 1M NaOH was then added slowly to adjust the pH of the solution to 10. To provide the capping agent to prevent agglutination, 6.34 g of trisodium citrate was added to stabilize the magnetite NPs. The magnetite NPs formed were then separated by centrifuging the mixture, and was subsequently dried. The chemical reaction for the co-precipitation of magnetite is shown below:

$$Fe^{2+}(aq) + 2Fe^{3+}(aq) + 8OH^{-}(aq) \rightarrow Fe_3O_4(s) + 4H_2O \qquad (l)$$

3.5 Synthesis of Magnetic Chitosan Hydrogel (MCH)

The chitosan synthesised in this study and commercial chitosan were both converted to MCH for comparison. Commercial chitosan is prepared using 80% (w/v) sodium hydroxide (Takarina et al., 2017) which is extremely corrosive and environmentally unfriendly. It is hence necessary to explore a greener method to produce chitosan which this study is exploring. Depending on the viscosity of the solution after the chitosan was dissolved, which in turn was dependent on the molecular weight of the chitosan, two different methods were adopted to synthesize MCH. Ethanol is able to precipitate solutions containing chitosan with high molecular weight (commercial chitosan), yielding MCH-E. On the other hand, NaOH is able to precipitate chitosan of low molecular weight (chitosan synthesised in this study), yielding

MCH-N. Coincidentally, the precipitation of magnetite is also induced by NaOH, thus the synthesis of MCH-N does not require the separate synthesis of magnetite NPs beforehand.

3.5.1 Synthesis of MCH by precipitation with Ethanol (MCH-E)

1.0g of chitosan was dissolved in 50 ml of 0.5M $FeCl_3$ solution, after which an equal mass of magnetite NPS was added to the solution and magnetically stirred for 30 min. Ethanol was then added to precipitate the MCH-E which was washed until it was free of Fe^{3+} ions. Crosslinking was carried out by submerging the MCH in 20ml of 5% (v/v) glutaraldehyde solution for 24 hours.

3.5.2 Synthesis of MCH by precipitation with NaOH (MCH-N)

3.87 g of iron(II) sulfate, 7.97 g of iron(III) chloride and 1.0g chitosan were dissolved in 50 ml of 0.5 M $FeCl_3$ solution. The mixture was heated to 80^{o}C for 30 min. pH of the solution was adjusted to 10 using 1M NaOH, after which 6.34 g of trisodium citrate was added and the solution was then stirred for 12 hours. The resulting MCH was obtained by centrifugation and crosslinking steps were carried out as mentioned in section 3.5.1.

3.6 Batch adsorption studies

To investigate the efficacy of the MCH synthesised, adsorption tests were carried out by adding 0.1g of adsorbent to 20 ml of dye solution of 50 ppm into a conical flask, and the mixture was agitated by the orbital shaker for 24 hours. The adsorbents were then magnetically separated and the resulting solution was analysed. Acid blue, direct red, and methyl orange solutions were analysed using a UV-VIS Spectrophotometer (Shimadzu UV 1800) at 565 nm, 526 nm and 462 nm respectively. The percentage of dye adsorbed was calculated using the following formula:

$$Percentage\ removed = \frac{Initial\ concentration - Final\ concentration}{Initial\ concentration} \times 100\%$$

3.7 Isotherm studies

Adsorption was carried out with 50 to 400 mg/L of acid blue and direct red dye and the equilibrium concentration data was fitted into the linearised forms of the Langmuir and Freundlich isotherms (Appendix, Pg 14-17). The adsorption capacity was obtained by the following formula:

$$Q\ (mg/g) = \frac{(C_i - C_f)(V)}{M}$$

where C_i = initial concentration in mg/l;
C_f = final concentration in mg/l;
V = volume of solution in dm^3.
M = **mass of MCH in g**

3.8 Kinetic studies

The order of reactions and the rate of adsorption of dyes were determined through kinetic studies. The adsorption of dyes was determined at various time intervals and the results were fitted to the pseudo first- and second-order equations (Appendix C, Pg 17).

3.9 Regeneration of MCH and reusability tests

Adsorption and regeneration of acid blue was repeated for 5 cycles. After each adsorption cycle, MCH was magnetically separated and washed with 1M NaOH, followed by deionized water until the colour of the dye was removed. To regenerate the hydrogel, 1M HCl was added.

4. Results and Discussion

4.1 Characterization of Chitosan synthesized

4.1.1 By FTIR

Percentage of deacetylation of the chitosan synthesized was determined from its FTIR spectrum (Appendix A, Pg 14) to be 41.3%, which was lower than that of the commercial chitosan, which was 80.0%, indicating that the binding of the chitosan to the central iron(III) ion may not be as strong as that in the commercial chitosan. This may results in lower adsorption capacity, as less sites are available for dyes to be adsorbed.

4.1.2 By Mass Spectrophotometry

Mass spectra reveal that the chitosan synthesized has a molecular weight of 800 - 900 Daltons, which is much lower than that of the commercially produced chitosan, which ranges from 30 000 – 150 000 Daltons. Thus, the chitosan synthesized would not be able to be precipitated by ethanol, due to the low molecular weight, and would have to be precipitated by NaOH as described in 3.5.2.

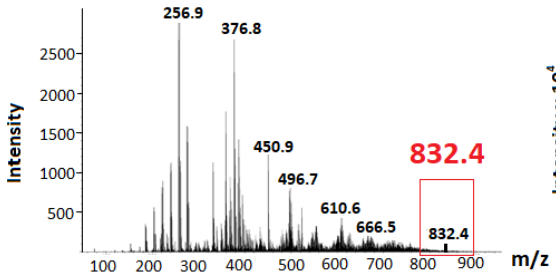

Figure 1(a): Mass spectrum (positive polarity) of chitosan synthesised

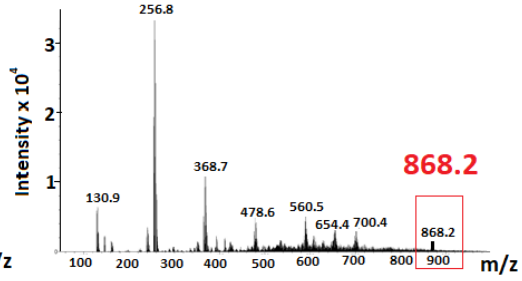

Figure 1(b): Mass spectrum (negative polarity) of chitosan synthesised

4.2 Characterization of MCH

4.2.1 By X-ray Diffraction (XRD)

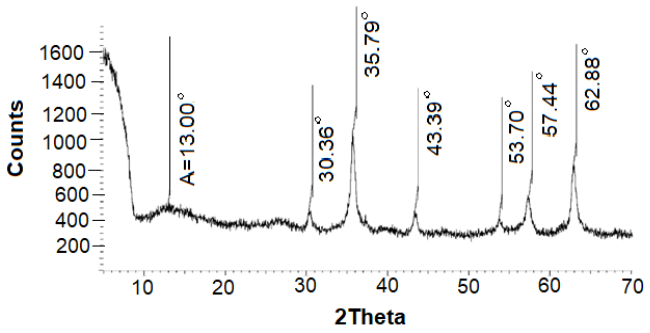

XRD spectrum of MCH-E (Figure 2) reveals sharp peaks at 30.36º, 35.79º, 43.39º, 53.70º, 57.44 and 62.88º, which are similar to that reported by Loh et al., (2008). This suggests that magnetite has been successfully incorporated into MCH-E.

Figure 2: XRD spectrum of MCH-E

4.2.2 By Scanning Electron Microscopy (SEM)

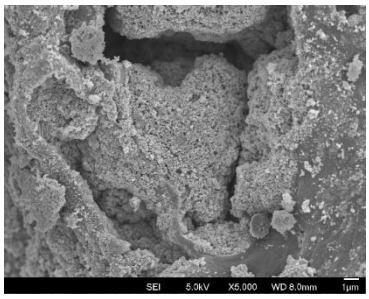

Figure 3: SEM image of MCH-N (x5000 zoom)

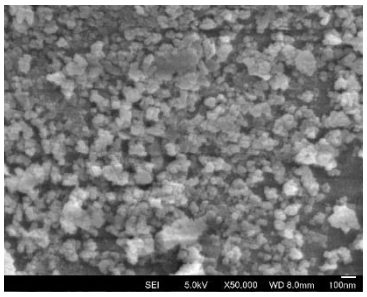

Figure 4: SEM image of MCH-E (x50000 zoom)

From the SEM images (Figure 3 and 4), it is observed that a layer of magnetite nanoparticles of 10 – 50 nm are coated onto the surface of the hydrogel, which allows it to be magnetic

4.3 Batch adsorption studies results

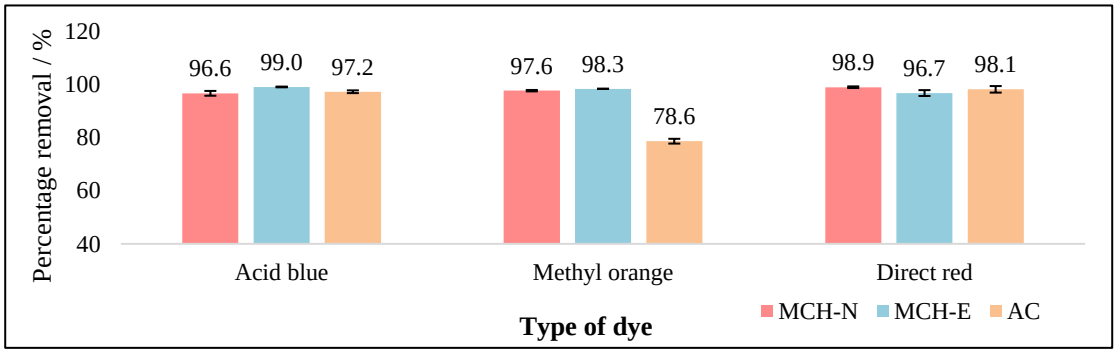

Figure 5: Results of adsorption tests. N=5

Adsorption tests show that both MCH-E and MCH-N have excellent percentage removal of more than 95% for all 3 dyes, while the commercial activated carbon (AC) pales in comparison in removing methyl orange. This stark difference between the performance of commercial AC and MCH in removing methyl orange is due to the difference in the mechanism

of adsorption of these two adsorbents. As suggested by the study of Lupul, Yperman, Carleer and Gryglewicz (2014), commercial activated carbon removes dyes mainly through pi-pi interactions between the aromatic rings of the dyes and the aromatic rings in the AC (Figure 6). Acid blue and direct red are easily removed by AC due to the large number of aromatic rings present in the organic dye, with 6 and 8 rings respectively. On the other hand, methyl orange only has 2 aromatic rings, explaining its low percentage removal by AC. MCH-N and MCH-E have a different adsorption mechanism. Acid blue, methyl orange and direct red are anionic dyes containing $-SO_3Na$ groups, which dissociate in water to form $-SO_3^-$. MCH adsorbs these dyes by allowing the dyes to act as ligands, binding to the central Fe^{3+} ion in the MCH complex (Figure 7), hence removing them from the solution.

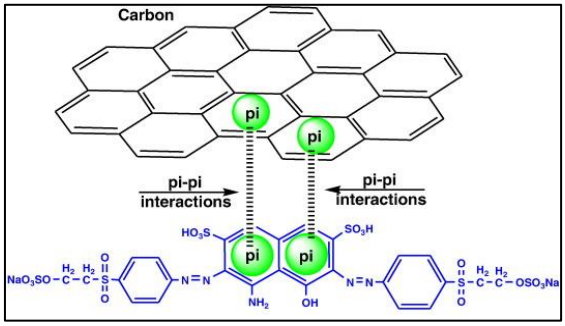

Figure 6: Interaction of AC with dyes

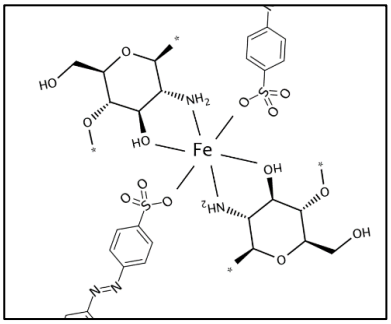

Figure 7: Interaction of MCH with dyes

4.4 Isotherm studies

Maximum adsorption capacity of both MCH-E and MCH-N derived from Langmuir isotherm studies (Appendix B, pg 14-17) on acid blue and direct red were compared with other studies, two of which were targeted at removing acid blue dye, while the other two were targeted at removing direct red dye (Table 1).

Table 1: Comparison of maximum adsorption capacity (q_m) of MCH with other adsorbents

Type of adsorbent	**Acid blue q_m / mg/g**	**Direct red q_m / mg/g**	**Reference**
MCH-E	169.5	153.8	This study
MCH-N	113.6	125.0	This study
Modified bentonite	45.0	-	Jeeva *et al*., 2018
Activated red mud	83.3	-	Shirzad *et al*., 2014
Activated rice husks	-	74.6	Safa *et al*., 2011
Cationized sawdust	-	68.5	Hebeish *et al*., 2011

MCH-E outperforms MCH-N in its maximum adsorption capacity (q_m) for both acid blue and direct red. Both MCHs outperform the adsorbents synthesised by several other researchers.

4.5 Kinetic studies

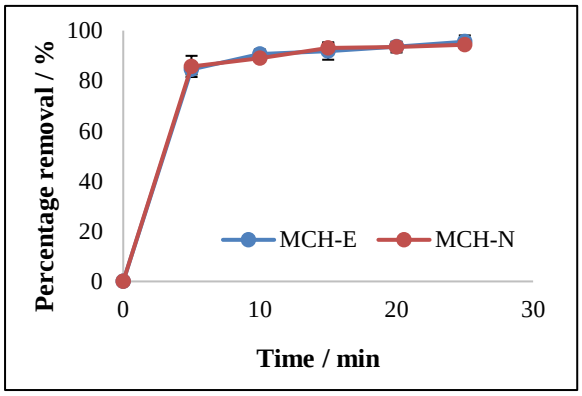

Figure 8: Kinetic studies on acid blue dye. N=5

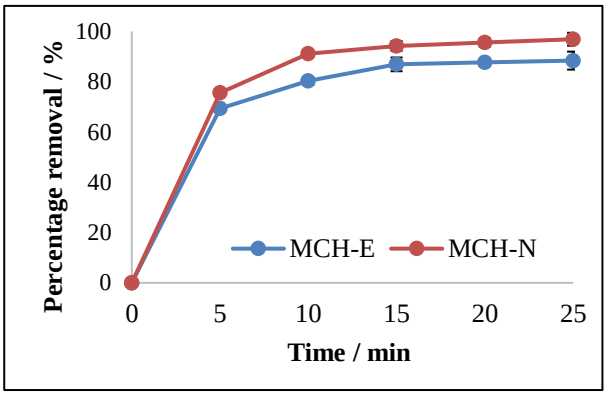

Figure 9: Kinetic studies on direct red dye. N =5

Kinetic studies reveal that both MCH-E and MCH-N were able to remove 80% of both direct red and acid blue dye within 10 min, which is rapid and efficient. For acid blue, both MCH-E and MCH-N had almost identical adsorption rates, while for direct red dye, MCH-N had a slightly more rapid removal compared to MCH-E. The data were fitted into the pseudo-first- and second-order kinetic equations to yield the rate constants and coefficient of determination (R^2).

Table 2: Rate constants of adsorption of dyes by MCHs

Type of adsorbent and pollutant	Pseudo-first-order constant / min^{-1}	R^2 value	Pseudo-second-order constant / g mg^{-1} min^{-1}	R^2 value
MCH-E | Direct Red	0.0425	0.8758	0.0949	0.9996
MCH-N | Direct Red	0.0960	0.9196	0.1035	0.9994
MCH-E | Acid blue	0.0576	0.9654	0.0983	0.9997
MCH-N | Acid blue	0.0475	0.9229	0.0971	0.9998

Table 2 reveals that R^2 for pseudo-second-order kinetic equation is greater, suggesting that all 4 kinetic studies had a better fit for the pseudo-second-order kinetic model, implying that the rate-limiting step is the surface adsorption that involves chemisorption.

4.6 Reusability tests

Results of the reusability tests on acid blue reveal that both MCH-E and MCH-N are able to sustain a percentage removal of more than 90% for at least 5 cycles, demonstrating their ability to be reused multiple times and still be effective in removing dyes from water. In cycle 5, the difference between the percentage removal of MCH-E and MCH-N has become significant (p-value of Mann-Whitney U test = 0.037 < 0.05), indicating that the binding of the dye onto MCH-N is stronger than that of MCH-E. Both MCH also have a significant drop in

performance after the first cycle (p-value of Mann-Whitney U test for MCH-E = 0.005 < 0.05, p-value of Mann-Whitney U test for MCH-N = 0.023 < 0.05), but still sustaining a high percentage removal.

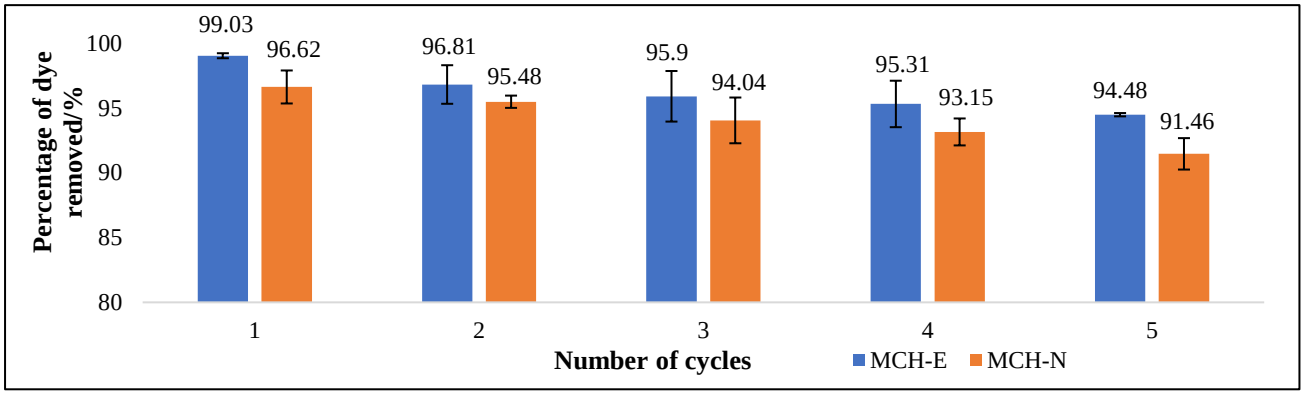

Figure 10: Reusability of MCHs in adsorbing acid blue. N=5

5. Conclusions and future work

MCH-E and MCH-N were successfully synthesized from commercial and synthesized chitosan respectively, with magnetite NPs coating the surface of both hydrogels. The effectiveness of MCH-E and MCH-N in removing acid blue and direct red was comparable to the commercial activated carbon, while the removal of methyl orange by both MCHs surpass that of commercial activated carbon. Both MCHs had a better fit for the Langmuir isotherm in the adsorption of direct red and acid blue, and the maximum adsorption capacities calculated from it surpasses the performance of several adsorbents synthesized by other researchers. Kinetic studies reveal that both MCH-E and MCH-N had extremely rapid rates of adsorption, removing 80% of both acid blue and direct red within 10 minutes. Both MCH-E and MCH-N fit the pseudo-second-order kinetic model, suggesting that the rate-limiting step is the surface adsorption that involves chemisorption. Both MCH-E and MCH-N can be reused and regenerated, consistently removing more than 90% of acid blue across 5 cycles of adsorption and regeneration.

In future, isotherm and kinetic studies can be extended to methyl orange. Adsorption of anions such as phosphate by MCH can be explored. It would also be interesting to investigate the effect of pH on adsorption of dyes by MCH. Mass of magnetite used in the synthesis may affect adsorption capacity and optimum mass of magnetite which results in greatest adsorption of MCH could be determined. Finally, it is important to determine if there is any significant leaching of iron from magnetite present in MCH as iron is a secondary pollutant.

References

Ado, A. Tukur, A.I., Ladan, M., Gumel, S.M., Muhammad, A.A., Habibu, S., & Koki, I.B (2015). A review on industrial effluents as major sources of water pollution in Nigeria. *Chemistry Journal*, 1(5), 159-164.

Avlonitis, S. A., Poulios, I., Sotiriou, D., Pappas, M., & Moutesidis, K. (2008). Simulated cotton dye effluents treatment and reuse by nanofiltration. *Desalination*, 221(1-3), 259-267.

Crini, G., & Badot, P. M. (2008). Application of chitosan, a natural aminopolysaccharide, for dye removal from aqueous solutions by adsorption processes using batch studies: A review of recent literature. *Progress in polymer science*, 33(4), 399-447.

Drahl, C. (2019). How seafood shells could help solve the plastic waste problem. *ScienceNews*. Retrieved from https://www.sciencenews.org/article/seafood-shells-chitin-plastic-food-waste

Giannakoudakis, D. A., Kyzas, G. Z., Avranas, A., & Lazaridis, N. K. (2016). Multi-parametric adsorption effects of the reactive dye removal with commercial activated carbons. *Journal of Molecular Liquids*, 213, 381-389.

Hebeish, A., Ramadan, M. A., Abdel-Halim, E., & Abo-Okeil, A. (2011). An effective adsorbent based on sawdust for removal of direct dye from aqueous solutions. *Clean Technologies and Environmental Policy*, 13(5), 713-718.

Jeeva, M., & Wan Zuhairi, W. Y. (2018, April). Adsorption of Acid Blue 25 dye by bentonite and surfactant modified bentonite. In *AIP Conference Proceedings* (Vol. 1940, No. 1, p. 020030). AIP Publishing LLC.

Kadirvelu, K., Kavipriya, M., Karthika, C., Radhika, M., Vennilamani, N., & Pattabhi, S. (2003). Utilization of various agricultural wastes for activated carbon preparation and application for the removal of dyes and metal ions from aqueous solutions. *Bioresource Technology*, 87(1),129-132.

Loh, K., Lee, Y., Musa, A., Salmah, A., & Zamri, I. (2008). Use of Fe3O4 Nanoparticles for Enhancement of Biosensor Response to the Herbicide 2,4-Dichlorophenoxyacetic Acid. *Sensors*, 8(9), 5775-5791. doi:10.3390/s8095775

Malik, R., Ramteke, D. S., & Wate, S. R. (2007). Adsorption of malachite green on groundnut shell waste based powdered activated carbon. *Waste Management*, 27(9), 1129-1138.

Mohan, N., Balasubramanian, N., & Basha, C. A. (2007). Electrochemical oxidation of textile wastewater and its reuse. *Journal of hazardous materials*, 147(1-2), 644-651.

Ngan, W. S.W., & Isa, I.M. (1998). Comparison study of copper ion adsorption on chitosan, Dowex A-1, and Zerolit 225. *J. Appl. Polym. Sci*, 67(6), 1067-1070.

Ngan, W. S.W., Teong, L.C., & Hanafiah, M. A.K.M. (2011). Adsorption of dyes and heavy metal ions by chitosan composites: A review. *Carbohydr Polym*, 83(4), 1446-1456.

Safa, Y., Bhatti, H. N., Bhatti, I. A., & Asgher, M. (2011). Removal of direct Red-31 and direct Orange-26 by low cost rice husk: Influence of immobilisation and pretreatments. *The Canadian Journal of Chemical Engineering*, 89(6), 1554-1565.

Sharma, M. K., & Sobti, R. C. (2000). Rec effect of certain textile dyes in Bacillus subtilis. *Mutation Research/Genetic Toxicology and Environmental Mutagenesis*, 465(1-2), 27-38.

Shen, D., Fan, J., Zhou, W., Gao, B., Yue, Q., & Kang, Q. (2009). Adsorption kinetics and isotherm of anionic dyes onto organo-bentonite from single and multisolute systems. *Journal of hazardous materials*, 172(1), 99-107.

Shirzad-Siboni, M., Jafari, S. J., Giahi, O., Kim, I., Lee, S. M., & Yang, J. K. (2014). Removal of acid blue 113 and reactive black 5 dye from aqueous solutions by activated red mud. *Journal of Industrial and Engineering Chemistry*, 20(4), 1432-1437.

Srivastava, V. C., Mall, I. D., & Mishra, I. M. (2007). Adsorption thermodynamics and isosteric heat of adsorption of toxic metal ions onto bagasse fly ash (BFA) and rice husk ash (RHA). *Chemical Engineering Journal*, 132(1-3), 267-278.

Sulak, M. T., Demirbas, E., & Kobya, M. (2007). Removal of Astrazon Yellow 7GL from aqueous solutions by adsorption onto wheat bran. *Bioresource technology*, 98(13), 2590-2598.

Takarina, N.D., Indah, A.B., Nasrul, A.A., Nurmarina, A., Saefumillah, A., Fanani, A.A., & Loka, K.D.P. (2017). Optimisation of deacetylation process for chitosan production from Red Snapper (Lutjanus sp.) scale waste. *Journal of Physics: Conference Series*, 812(1), 012110. DOI: 10.1088/1742-6596/812/1/012110

Toliba, A. O., Rabie, M. A., & El-Araby, G. M. (2014). Extending the shelf-life of cold-stored strawberry by chitosan and carnauba coatings. *Zagazig Journal of Agricultural Research*, 41(5), 1067-1076.

Zhu, H. Y., Jiang, R., Fu, Y.Q., Jiang, J. H., Xiao, L., & Zeng, G.M. (2011). Preparation, characterisation and dye adsorption properties of γ-Fe2O3/SiO2/chitosan composite. *Appl. Surf. Sci*., 258(4), 1337-1344.

Appendix A: FTIR of chitosan synthesized

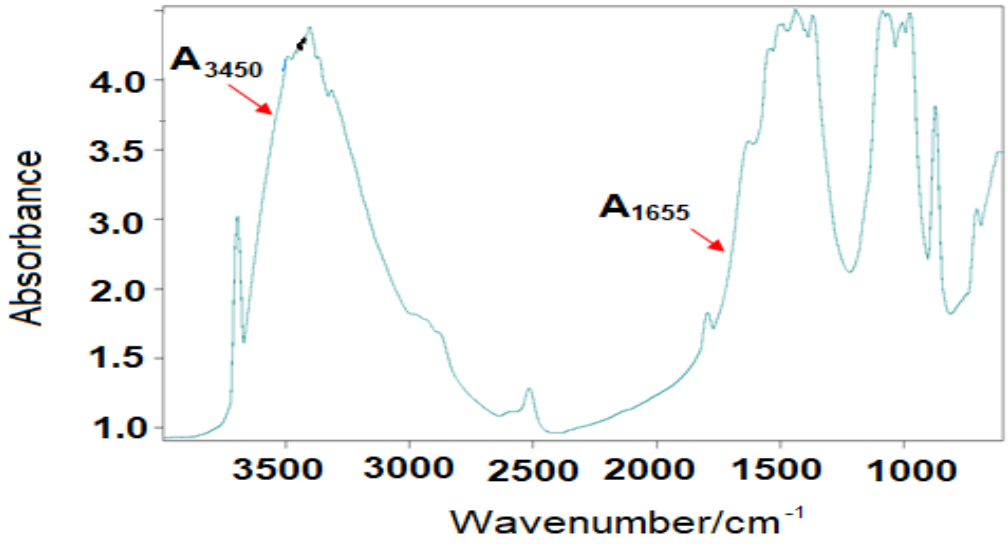

Figure 11: FTIR spectrum of chitosan synthesised

The percentage of deacetylation (DDA) of the chitosan synthesized was determined by the following formula:

$$DDA(\%) = [1- (A_{1655}/ A_{3450})/1.33] \times 100$$

Using FTIR software, A_{1655} and A_{3450} were determined to be 2.88 and 3.69 respectively. DDA(%) was hence calculated to be 41.3%

Appendix B: Langmuir and Freundlich isotherm

The equilibrium concentration data obtained from initial concentration tests on acid blue and direct red were fitted into Langmuir isotherm and Freundlich isotherm. The Langmuir isotherm assumes that the adsorbed material (such as acid blue) is adsorbed over a uniform adsorbent surface at a constant temperature.

The linear form of Langmuir isotherm equation is given by:

$$\frac{C_e}{q_e} = \frac{1}{bq_m} + \frac{C_e}{q_m}$$

Where Ce is the equilibrium concentration of dye (mg/L), qe is the equilibrium capacity of the sorbents (mg/g), b is the Langmuir constant that indicates the sorption intensity and qm is the maximum sorption capacity (mg/g).

The Freundlich isotherm assumes that the adsorption occurs on a heterogeneous surface. The linear form of Freundlich equation is given by:

$$log(Q_e) = log(K_F) + \frac{1}{n} log(C_e)$$

Where Ce is the equilibrium concentration of dye (mg/L), Qe is the equilibrium capacity of the sorbents (mg/g), K_F, a constant, is related to sorption capacity and n corresponds to sorption intensity.

The Langmuir and Freundlich isotherm plots are shown below:

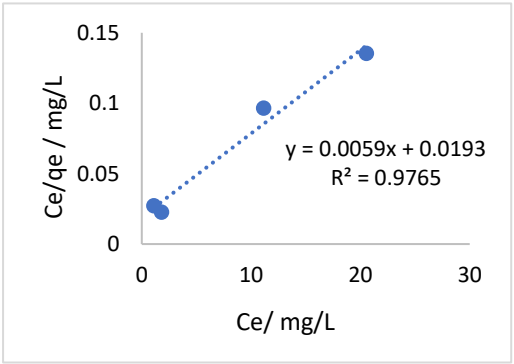

Figure 12: Langmuir isotherm fit of removal of acid blue by MCH-E

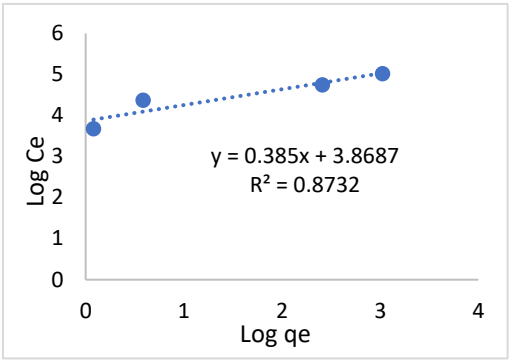

Figure 13: Freundlich isotherm fit of removal of acid blue by MCH-E

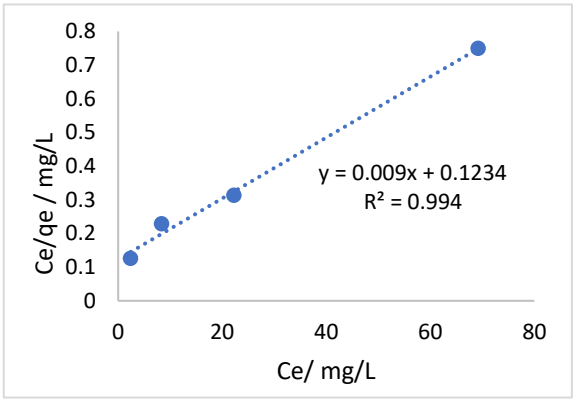

Figure 14: Langmuir isotherm fit of removal of acid blue by MCH-N

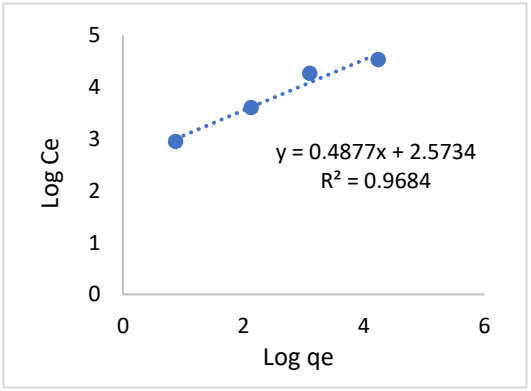

Figure 15: Freundlich isotherm fit of removal of acid blue by MCH-N

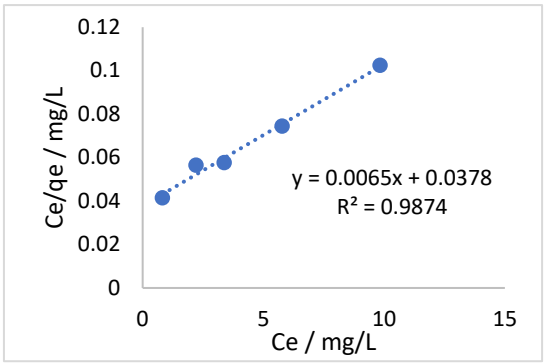

Figure 16: Langmuir isotherm fit of removal of direct red by MCH-E

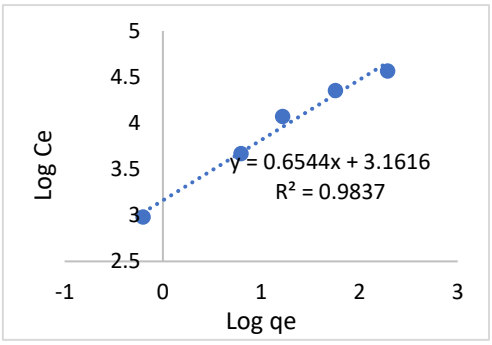

Figure 17: Freundlich isotherm fit of removal of direct red by MCH-E

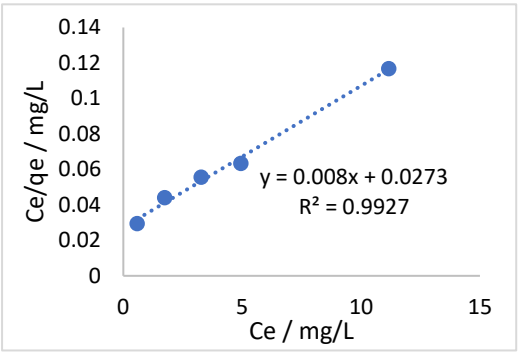

Figure 18: Langmuir isotherm fit of removal of direct red by MCH-N

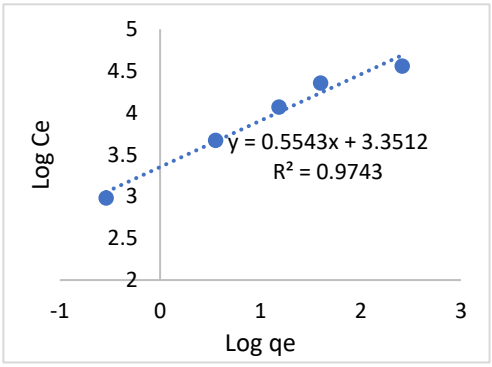

Figure 19: Freundlich isotherm fit of removal of direct red by MCH-N

If the equilibrium concentration data fits the Langmuir isotherm, adsorption can be inferred to be monolayer. Important information such as the maximum adsorption capacity of the MCH can be derived from the inverse of the gradient of Langmuir linear equations.

In contrast, if the equilibrium concentration data fits the Freundlich isotherm, adsorption can be inferred to occur on a heterogeneous surface and adsorption is multilayer. A comparison between the R^2 values of the graph can determine which model the data set fits better (Table 3).

Table 3: R^2 value comparison of Langmuir and Freundlich isotherms

	Acid blue		Direct red	
Adsorbent	R^2 value for Langmuir isotherm	R^2 value for Freundlich isotherm	R^2 value for Langmuir isotherm	R^2 value for Freundlich isotherm
MCH-E	0.9765	0.8732	0.9927	0.9743
MCH-N	0.9940	0.9684	0.9874	0.9837

All data sets had a better fit for the Langmuir isotherm, implying that the MCH has a homogenous surface with monolayer adsorption.

Appendix C: Adsorption Kinetic Models

The adsorption kinetic models, namely, the pseudo-first-order and pseudo-second-order, are useful for determining whether physical or chemical adsorption process occurs. If the pseudo-first-order model provided better fit result, then the adsorption is a physical process. On the other hand, if the pseudo-second-order model fits better, adsorption is a chemical process.

The kinetic studies data was fitted to pseudo-first- and second-order equations. The first-order equation is described by:

$$\ln(q_e - q_t) = \ln q_e - k_1 t$$

Where q_e is the equilibrium concentration,

q_t is the concentration at time t,

t is the time elapsed and

k_1 is the pseudo-first-order constant

The second-order equation is described by:

$$\frac{t}{q_e} = \frac{1}{k_2 q_e^2} + \frac{1}{q_e} t$$

Where q_e is the equilibrium concentration,

t is the time elapsed and

k_2 is the pseudo-second-order constant